Cure Behavior of UP/Org-MMT/MEKP/Cobalt Octoate Nanocomposites by the Dynamic Torsional Vibration Method

Yiyun Cheng, Dazhu Chen, Chunlei Wang, Pingsheng He

Department of Polymer Science and Engineering, University of Science and Technology of China, Hefei, 230026, Anhui, China

Received 18 December 2003; accepted 27 August 2004
DOI 10.1002/app.21605
Published online in Wiley InterScience (www.interscience.wiley.com).

ABSTRACT: The cure behavior of unsaturated polyester(UP)/organo-montmorillonite (Org-MMT)/methyl ethyl ketone peroxide (MEKP)/cobalt octoate intercalated nanocomposites at varying temperatures and Org-MMT loadings was investigated by the Dynamic Torsional Vibration Method (DTVM). The apparent kinetic parameters of the cure reaction, including the gelation time t_g, apparent activation energy E_a, and curing rate, etc., were estimated by Flory's gelation theory, non-equilibrium thermodynamic fluctuation theory, and Avrami equation. The theoretical prediction is in good agreement with the experimental results obtained by the DTVM. The gelation time t_g increases, and the rate of curing reaction decreases, with increasing Org-MMT loadings, but there is no obvious effect of Org-MMT on the apparent activation energy E_a and the curing process of nanocomposites. A two-step cure process of UP was observed due to the addition of Org-MMT. © 2005 Wiley Periodicals, Inc. J Appl Polym Sci 97: 1–7, 2005

Key words: unsaturated polyester; nanocomposite; gelation time; Flory's theory; Avrami equation

INTRODUCTION

A great deal of attention has been paid to the organic–inorganic hybrid nanocomposite recently.[1–3] The nanocomposite is not the simple mixture of organic polymer matrix and inorganic filler only, but is a composite in which two components disperse into one another in nanometer scale. The nano- scale effect leads to strong interfacial interactions and exhibits many positive physical and mechanical properties of nanocomposites. In general, the dispersion of clay particles in a polymer matrix can result in the formation of three general types of composite: (a) conventional composites; b) intercalated composites formed by the insertion of polymer molecules into the clay host galleries (although the basal spacing rises, the clay remains in a regular gallery structure); and (c) exfoliated nanocomposite, in which the individual 10 Å thick silicate layers are dispersed in a polymer matrix and segregated from one another, and the gallery structures are completely destroyed. Lots of reports about the layer silicate–epoxy nanocomposite and the epoxy– clay nanocomposite can be found in the literature.[4–6] However, no report, to the authors' knowledge, could be found on the cure process *in situ* of the unsaturated polyester (UP)–clay system in the literature.

Curing of a resin system is the critical and productivity controlling step in the fabrication of the thermosetting-matrix composites. However, the cure process of an epoxy resin is the crosslinking of linear macromolecules with a complicated mechanism. As soon as the crosslinking forms, the resin will not be softened and melted, leading to a difficulty to study. Traditionally, chemical analysis, Fourier transformed infrared spectroscopy,[7] and differential scanning calorimetry [8,9] detecting the degree of conversion of reaction groups were used to study the cure process. The sensitivity and function of these analysis techniques are much reduced at the last curing stage due to the increased consumption of reactive groups. The cure process can be studied successfully by mechanical methods, and the dynamic torsional vibration method (DTVM) developed in our lab has successfully been used to investigate the cure behavior in several resin systems.[10–17]

In this presentation, the cure behavior of UP/Org-MMT/MEKP nanocomposites was studied with the DTVM. The apparent kinetic parameters of the cure reaction, including the gelation time t_g, apparent activation energy, and curing rate, etc., were estimated by Flory's gelation theory, non- equilibrium thermodynamic fluctuation theory, and Avrami equation. The effect of Org-MMT loading on the cure process was studied as well.

EXPERIMENTAL

Materials

Na^+-montmorillonite with a cation exchange capacity value of about 100 mmol/100 g was purchased from

Correspondence to: P. He (hpsm@ustc.edu.cn)

Qingshan Chemistry Agent Factory in Lin'an, China. Unsaturated polyester resin was donated by the Glass Fiber Reinforced Plastic Factory in Anhui. Methyl ethyl ketone peroxide (MEKP), produced in Huifeng Chemistry Agent Material Factory in Jiangyin, China, was used as curing agent. The surfactant of clay, $(CH_3)_3(CH_2)_{16}NH_4Br$, was purchased from the Research Institute of Xinhua Active Material in Changzhou. The organo-montmorillonite (Org- MMT) was prepared by ion exchange.

For the isothermal cure experiment, UP, the initiator MEKP, and its promoter of cobalt octoate were mixed in the stoichiometric ratio of 100 : 2 : 0.15 (by weight). Then, the mixture was mixed with Org-MMT powder with the loadings of 0, 2, 5, and 7phr, respectively.

Ion exchange process

Na^+-montmorillonite was added to a three-necked 1000 mL round-bottom flask loaded with distilled water, and mixed using a mechanical stirrer equipped with a glass stirring rod in room temperature; 30 g $(CH_3)_3(CH_2)_{16}NH_4Br$ per hundred grams clay by weight was added and placed in a 90° water bath for 2 h. The exchanged clays were washed with deionized water until no bromide was detected with 0.1*N* $AgNO_3$ solution and dried in the air. The clays were ground with a mortar and pestle, and the 40–60_m fraction was collected. The product made in this way was identified as 16-Mont [11].

X-ray diffraction (XRD)

The lattice spacing of montmorillonite was measured by a Rigaku D/max-γB X-ray diffractometer with the CuK_α line (λ = 0.1542 nm), a tube voltage of 40 kV, and a tube current of 100 mA. The scanning range is from 2.2° to 10° with a rate of 2°/min.

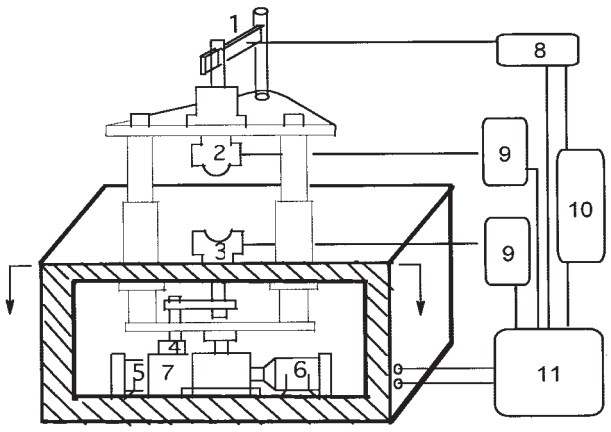

Figure 1 Schematic representation of the dynamic torsional vibration apparatus.

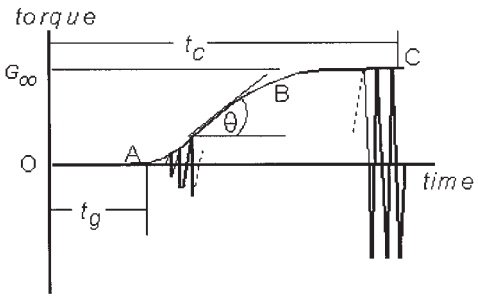

Figure 2 Analysis of isothermal cure curve.

Dynamic torsional vibration method and experimental curve analysis

Dynamic torsional vibration is a non-resonant forced vibration. The schematic diagram of a homemade experimental setup-HLX-I Resin Curemeter is shown in Figure 1. The lower mold **3,** having a heater within it and used as the torsional vibrator, is filled with the resin materials. When the motor **6** is switched on, the upper mold **2,** having a heater within it too, comes down, and the molds close with a gap that can be adjusted. The cure temperature is controlled with thermistors. Thus, the isothermal cure process can be performed. As soon as the upper and lower molds close, the motor **5** is on, and the lower mold starts a torsional vibration with a frequency of 0.05Hz at an angle below 1°, which also can be adjusted according to the hardness of the cured resin materials, by means of ecentric disc 4 on the speed change gear **7.** The torque amplitude of the torsional vibration is transformed into electric signals by means of the strain gauge load cell **1,** amplified through the amplifier **10** and recorded by the recorder **11.** The UP resin system with a different degree of cure has a different torque (or viscosity, modulus, etc.). Therefore, the change in the mechanical properties, that is, the degree of cure of the resin system, can be monitored and determined by measuring the changes in torque, and a continuing curve reflecting the whole cure process can be obtained.

The typical experimental curve obtained by the dynamic torsional vibration apparatus is shown in Figure 2. The abscissa is the curing time, and the ordinate is the torque required to turn the resin system by a small angle, which corresponds to the modulus or viscosity of the resin system, and can be thought of as a relative parameter of the degree of cure. The time of closure of the molds is taken as the starting time of cure point O. In the range of OA of the curing time, the network structure formed during the cure reaction is not enough to cause forced vibration of the upper mold. As a result, the strain gauge load cell will not have any signal to input, so that the experimental curve is a linear line corresponding to the abscissa. At point A, the viscosity of the resin system is high enough (i.e., the network formed is complete enough)

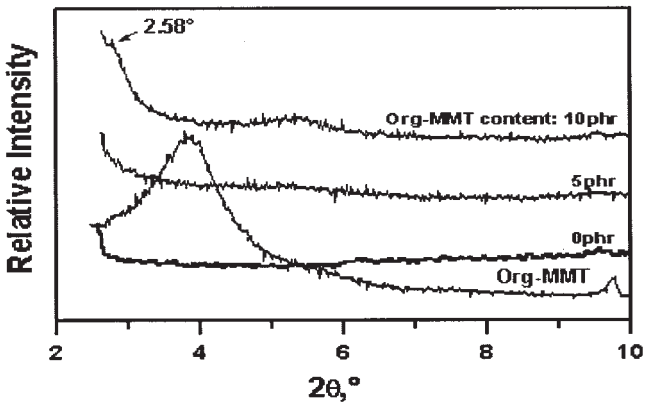

Figure 3 XRD patterns of UP/Org-MMT/MEKP/cobalt octoate system.

for the gelation in the resin system to occur, and the torque appears and the strain gauge load cell inputs some signal. Thus, point A is the gel time t_g for the resin system. After point A, the torque increases with increasing of the curing time. The increasing amplitude of the torque (slope of the curve) reflects the rate of the curing reaction. The increasing trend of the torque tends to steady with increasing curing time, and the equilibrium torque G_∞ is thus reached (point C). In the meantime, the curing reaction is completed and a cup-like experimental curve is obtained. The envelope of the experimental curve corresponds to the change of mechanical behavior of the resin system during cure. Since the cup-like experimental curve is symmetric to the time axis, for convenience we can just take the upper- half of the envelope as the isothermal cure curve to analyze the cure process.

RESULTS AND DISCUSSION

X-ray diffraction analysis

X-ray diffraction (XRD) patterns for UP/Org-MMT/MEKP/cobalt octoate nanocomposites with varying Org-MMT loadings cured at a temperature of 100° are shown in Figure 3. The XRD patterns can reveal the change of the lattice spacing of Org-MMT after the cure of the UP/Org-MMT mixture. Generally, for intercalated nanocomposites the lattice spacing increases, but Bragg diffractions still exist in the diffractogram, which shifted to a lower angle. If the lattice spacing continues to increase, an exfoliated nanocomposite is formed, leading to the disappearance of the Bragg diffraction.[18] The (001) diffraction peak exists in $2\theta = 3.88°$, related to the d-spacing of 22.7 Å; while for the nanocomposites, a lower (001) diffraction peak ($2\theta = 2.58°$) and higher d-spacing ($d = 34.2$ Å) were examined. That is, as a function of the insertion of the polymer chains into montmorillonite galleries and of the polymerization force, the spacings of montmorillonite, almost independent of its content, expand evidently. The existence of a (001) diffraction peak with an increase of gallery spacing is indicative of the formation of interclated layered silicate nanocomposites.

The isothermal cure curve

The isothermal cure curves of the UP/Org-MMT/MEKP/cobalt octoate nanocomposites with Org-MMT loadings of 0, 2, 5, and 7phr at temperatures of 20, 30, 40, and 50° a shown in Figure 4. Most of the cure curves have similar shape, but obvious differences in gelation time t_g, cure rate, and maximum torque could be observed. It is obvious from Figure 4 that the gelation time decreases and the cure reaction will be faster and faster with the increasing of temperature. Same as the temperature dependence, the t_g decreases with increasing of Org-MMT loadings, which occurs especially beyond the loading of 5phr. The same phenomenon could also be found in ref. 17. The t_g obtained from Figure 3 and some related parameters a listed in Table I.

Flory's gelatin theory

According to Flory's gelation theory,[19] the chemical conversion at the gel point of the resin system is constant and is not related to the reaction temperature and other experimental conditions. As a result, the apparent activation energy of cure reaction E_a can be calculated from gel time t_g:

$$\ln t_g = C + E_a/RT \tag{1}$$

where T is the curing temperature (K); R, the gas constant; and C, a constant. Figure 5 shows a plot of $\ln t_g$ versus $1/T$ for the nanocomposites with various Org-MMT loadings. The apparent activation energy E_a can be calculated from the slope of the lines. The ideal linearity demonstrates that Flory's theory is appropriate for the cure process.

Nonequilibrium thermodynamic fluctuation theory

Hsich's non-equilibrium thermodynamic fluctuation theory,[20–22] by which we predicted the cure behavior of our experimental systems, directly describes the changes of physical or mechanical properties. Hsich considered that there are similarities between the dynamic process of resin curing and the process of a molecular structure becoming floppy,[20] so one can use a function related with the time to describe the variation of physics' mechanical properties in the curing system. The curing reaction can be regarded as many chemical reaction units, and each unit is related with a dynamic ordered parameter. According to the theory, the physical or mechanical properties of the UP resin system during cure can be expressed as:

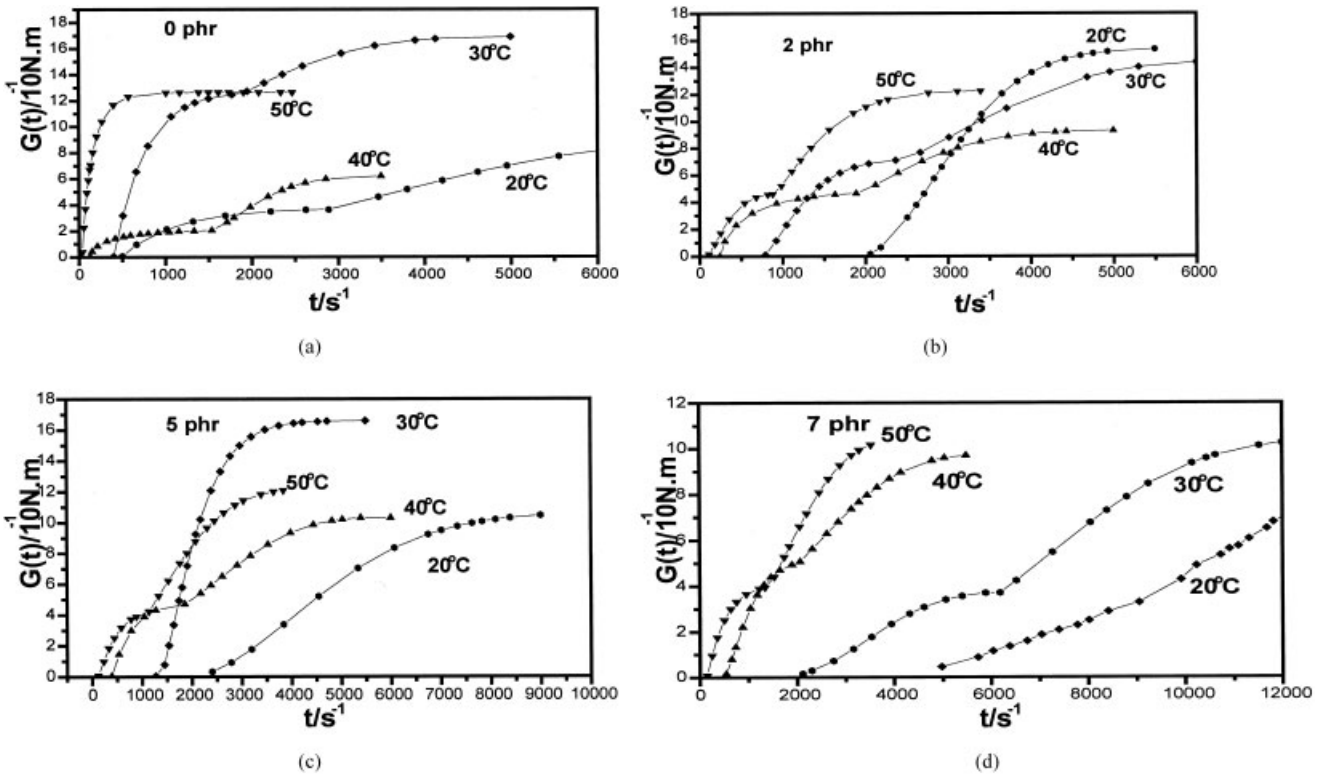

Figure 4 Cure curve of UP/Org-MMT/MEKP/cobalt octoate system at various temperatures: (a) 0 phr, (b) 2 phr, (c) 5 phr, and (d) 7 phr.

$$\frac{G_\infty - G(t)}{G_\infty - G_0} = \exp\left[-\left(\frac{t}{\tau}\right)^\beta \right] \tag{2}$$

where G_∞ and G_0 are the final and initial physical and mechanical quantities (torque or modulus, viscosity, etc.) during cure, respectively; $G(t)$, the property at time t; τ, the time parameter (relaxation time) of the reaction system; and β, the constant describing the width of the relaxation spectrum.

In our experiment, the mechanical quantity is torque. As seen from the isothermal cure curve in Figure 4, G_0 is zero, the torque beginning to appear only after the gel time t_g. Eq. (2) describing the curing curve after t_g would be

TABLE I
Kinetic Parameters for the UP/Org-MMT/MEKP/Cobalt Octoate Systems

Org-MMT	T(°C)	G_∞	t_g(s)	τ(s)	β	n	k
0 phr	50	12.62	38.1	124.1	0.88	0.87	1.53E-02
	40	6.27	130.6	374.8	0.68	0.70	2.43E-02
	30	16.90	400.4	1042.9	1.03	1.04	2.13E-03
	20	9.36	587.3	4103.7	0.96	0.97	1.87E-03
2 phr	50	7.63	88.6	388.4	1.42	1.43	5.16E-04
	40	9.32	244.9	613.0	0.75	0.76	1.13E-02
	30	14.45	766.5	1334.6	1.35	1.34	1.99E-04
	20	15.38	1952.2	3288.0	1.80	1.78	2.76E-06
5 phr	50	12.36	119.3	416.3	1.24	1.31	5.21E-04
	40	10.36	390.5	765.7	1.04	1.02	2.20E-02
	30	16.67	1254.6	2281.6	1.33	1.36	1.16E-02
	20	10.84	2547.8	5225.7	1.75	1.80	5.04E-07
7 phr	50	10.41	144.5	158.2	1.07	1.08	1.65E-03
	40	9.75	499.9	367.5	1.36	1.52	1.57E-04
	30	10.4	1465.1	757.2	2.33	2.28	1.75E-08
	20	7.13	4203.0	1073.9	2.43	2.42	9.35E-10

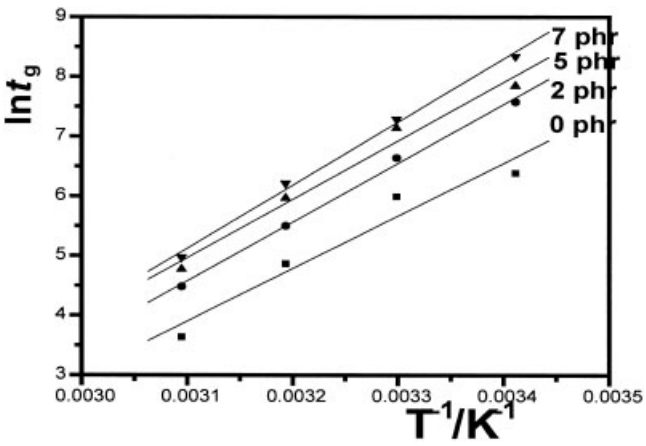

Figure 5 Plots of $\ln t_g$ versus $1/T$ for UP system with different Org-MMT fillers.

$$\frac{G_\infty - G(t)}{G_\infty} = \exp\left\{ -\left[\left(\frac{t - t_g}{\tau}\right)^\beta\right]\right\} \tag{3}$$

Eq. (3) describes the changes in the torque of the resin system during cure in which t_g and G_∞ can be read directly from the isothermal cure curve.

In order to obtain the relaxation time τ let $t = t_g + \tau$, thus:

$$G(t) = G(t_g + \tau) = G_\infty(1 - e^{-1}) = 0.63G_\infty \tag{4}$$

From a measurement of time corresponding to 0.63 G_∞ in the experimental curing curve, the relaxation time τ can be obtained by Eq. (5):

$$\tau = t - t_g \tag{5}$$

Having determined τ, eq. (3) is reduced to an equation with a single parameter β only. A non-linear regression is used to fit Eq. (3) to all experimental cure curves. The values of β at various temperatures or Org-MMT loadings can be determined by using the line of best fit. With this β value, the torque *G(t)* at any time, that is, the theoretically predicted value, can be calculated according to Eq. (3) provided that the gel time t_g and the relaxation time τ are already known.

Analysis of cure curves with the Avrami equation

The Avrami theory is most often used to describe the kinetic process of polymer crystallization. Since many molecular aggregates (microgels) or high-molecular-weight particles have been observed during an infinite network formation as a result of crosslinking,[23], Lu[24] considered that in a broad sense, crystallization can be considered as a physical form of crosslinking and in some aspects the behavior of amorphous crosslinking polymers is similar to that of crystals. Therefore, it is possible to predict the cure process of thermosets using the Avrami equation. The cure kinetics of the epoxy resin[24,25] and unsaturated polyester[26] have been analyzed with the Avrami equation earlier, and good agreement between the theoretical predictions and the experimental DSC data was achieved.

The relative degree α of cure at t time can be calculated according to the curing curve as follows:

$$\alpha = G(t)/G_\infty \tag{6}$$

and the isothermal curing curves can be changed into the relationship between the degree of cure α and the curing time $(t - t_g)$ after the gel point. The isothermal cure process can be analyzed using the following modified Avrami equation 27:

$$\alpha = 1 - \exp\,[\,-k(t - t_g)^n] \tag{7}$$

or

$$\ln[\,-\ln(1 - \alpha)] = n\ln(t - t_g) + \ln k \tag{8}$$

where n is the Avrami exponent that is a reflection of the nucleation and growth mechanisms, and k is a temperature dependent kinetic constant.

The plots of $\ln[-\ln(1-\alpha]$ versus $\ln(t-t_g)$ for the data obtained on the cure process of UP/Org- MMT/MEKP/cobalt octoate are shown in Figure 6. The results treated by the Avrami equation are reported in Table 1. The good linearity justifies that it is valid to illustrate the cure process after t_g by the Avrami equation. Meanwhile, it is found that the values of kinetic constant k increased as the cure temperature increased, that is, the higher temperature, the faster the cure rate, which is in good agreement with the general rule of chemical reactions.

The activation energy can also be estimated by the Avrami method. An empirical approach can be used to describe the temperature dependence of kinetic constant *k.* Assuming that k is thermally activated[22]:

$$k^{1/n} = A\exp\,(\,-E_a/RT) \tag{9}$$

or

$$n^{-1}\ln k = \ln A - E_a/RT \tag{10}$$

where E_a is an activation energy associated with the cure process, and A is a pre-exponential constant. The logarithmic plots of $n^{-1}\ln k$ as a function of $1/T$ are shown in Figure 7. The good fit to linearity allows calculation of the activation energy from the slope of the straight line.

The values of the activation energy obtained by the above two methods are listed in Table II. We can find out that the values of activation energy became higher as the concentration of Org-MMT increased. Obviously, the differences between one another are not

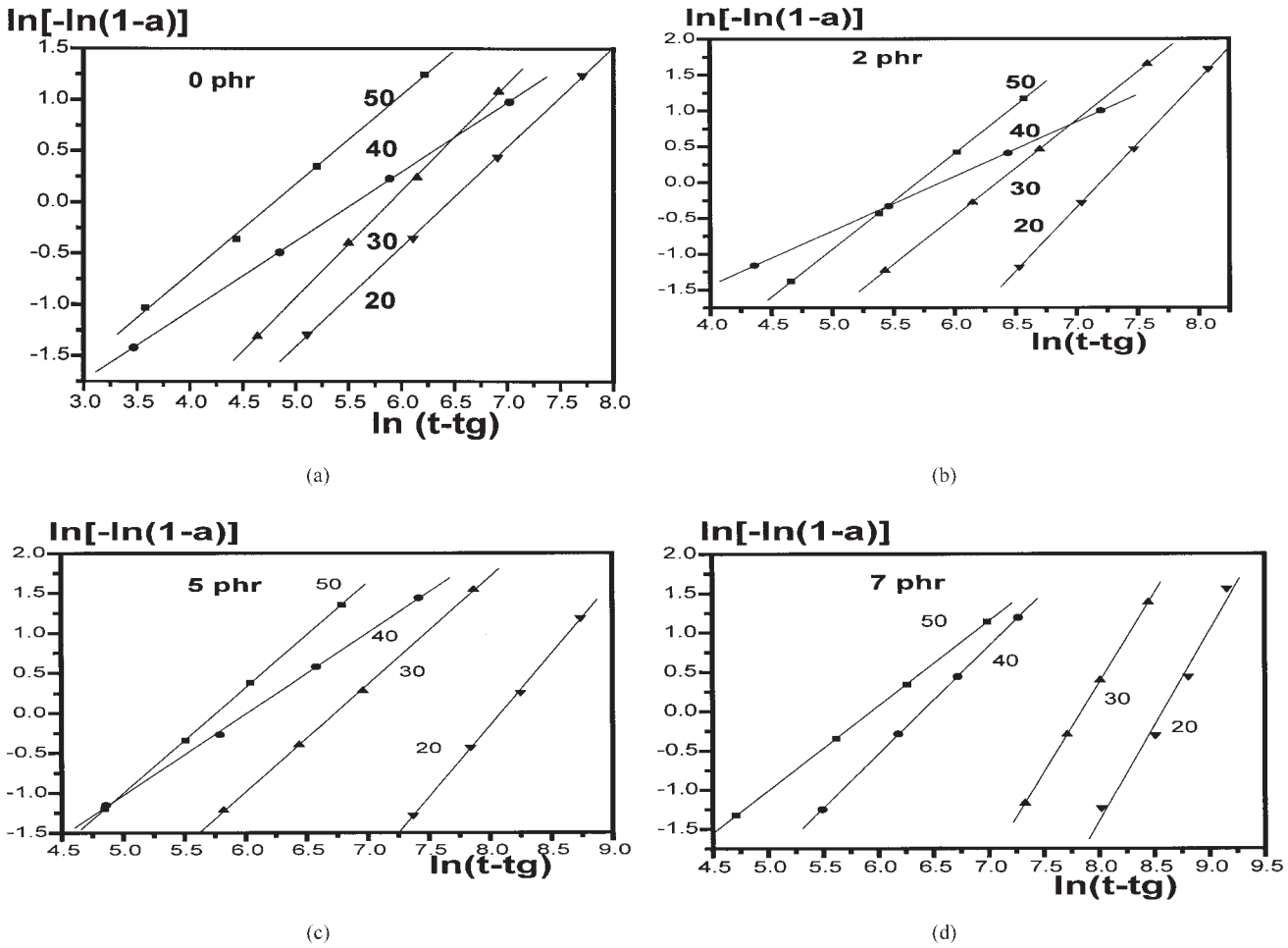

Figure 6 Avrami plots of ln $[-ln(1-a)]$ versus $ln(t-t_g)$ of UP system with different Org- MMT fillers: (a) 0 phr, (b) 2 phr, (c) 5 phr, and (d) 7 phr.

insignificant. The reason may be attributed to the existence of different mechanisms at various cure stages. Before (or at) the gel point, the polymerization is kinetic-controlled and the cure reaction is relatively easy. After the gel point, the cure reaction is predominantly diffusion-controlled as the retardation of viscosity and a mass dispersion limitation eventually set in, and the cross-linking reaction of unsaturated polyester resin becomes more difficult. Therefore, the activation energies at the gel point obtained from the gelation time are distinctly higher than those after the gel point obtained from the apparent rate constant.

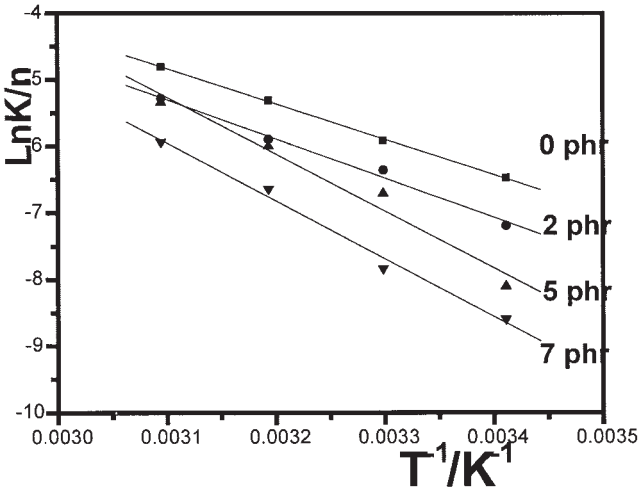

Figure 7 Plots of $1/n\ln k$ versus $1/T$ of UP/ Org-MMT/ MEKP/cobalt octoate system.

TABLE II
Activation Energy of Epoxy UP/Org-MMT/MEKP/Cobalt Octoate Systems

Loadings (phr)	E_a (kJ/mol)	E_a* (kJ/mol)
0	73.38	44.21
2	81.98	47.35
5	81.48	71.04
7	87.96	72.16

E_a and E_a* are the apparent activation energies obtained from Flory's theory and the Avrami equation, respectively.

CONCLUSION

The Dynamic Torsional Vibration Method investigated the cure behavior of UP/Org- MMT/MEKP/ cobalt octoate intercalated nanocomposites with different Org-MMT loadings. From the experiment, we conclude: Temperature increase reduces the gel time t_g, and increases the cure rate and the value of k; and the addition of organo-montmorillonite reduces the cure rate of UP to a considerable extent. The addition of Org-MMT has no considerable effect on the apparent activation energy of the cure reaction, judging from the similarity of cure curves with and without Org-MMT, Org-MMT has no specific effects on the formation of the nanocomposites. Also, the prediction based on Flory's gelation theory, the non-equilibrium thermodynamic fluctuation theory, and the Avrami equation is in ideal agreement with the experimental results, which verifies the theory in a reverse way. We observed twi-cure under most experimental conditions, but the ultimate cause of this phenomenon needs further exploration.

References

1. Gao, Z. W.; Zhao, X. P. Polymer 2003, 44, 4519.
2. Ma, J.; Xu, H.; Ren, J. H. Polymer 2003, 44, 4619.
3. Xu, W. B.; He, P. S.; Chen, D. Z. Eur Polym J 2003, 39, 617.
4. Chen, C. G.; Khobaib, M.; Curliss, D. Progress in Organic Coatings 2003, 47(3–4), 376.
5. Ratna, D.; Becker, O.; Simon, G. P. Polymer 2003, 44, 7449.
6. Becker, O.; Varley, R.; Simon, G. P. Polymer 2002, 43, 4365.
7. Sacher, E. Polymer 1973, 14, 91.
8. Bajaj, P.; Jha, N. K.; Kumar, R. M. J Appl Polym Sci 1990, 40, 203.
9. Ooi, S. K.; Cook, W. D.; Simon, G. P.; Such, C.H. Polymer 2000, 41, 3639.
10. Xu, W. B.; Liang, G. D.; Wang, W. J Appl Polym Sci 2003, 88, 3093.
11. Xu, W. B.; Bao, S. P.; He, P. S. J Appl Polym Sci 2002, 84, 842.
12. Chen, D. Z.; He, P. S.; Pan, L. J. Polym Test 2003, 22, 689.
13. Chen, D. H.; He, P. S. J Compos Mater 2003, 37, 1275.
14. He, P. S.; Li, C. E. J Appl Polym Sci 1991, 43, 1011.
15. Zou, G.; Fang, K.; Sheng, X. Chem J Chinese U 2003, 24, 537.
16. Zhou, Z. Q.; Jin, B. K.; He, P. S. J Appl Polym Sci 2002, 84, 1457.
17. Xu, W. B.; He, P. S. Acta Polym Sin 2001, 5, 629.
18. Wang, Z.; Lan, T.; Pinnavaia, T. J. Chem Mater 1996, 8, 2200.
19. Flory, P. J. Principles of Polymer Chemistry; Cornell University Press: New York, 1953; p 353.
20. Hsich, H. S. -Y. J Appl Polym Sci 1982, 27, 3265.
21. Avrami, M. J Chem Phys 1939, 8, 212.
22. Cebe, P.; Hong, S. D. Polymer 1986, 27, 1183.
23. Pollard, M.; Kardos, J. L. Polym Eng Sci 1987, 27, 829.
24. Lu, M. G.; Shim, M. J.; Kim, S. W. Mater Sci Commun 1998, 56, 193.
25. Kim, S. W.; Lu, M. G.; Shim, M. J. Polym J 1998, 30, 90.
26. Lu, M. G.; Shim, M. J.; Kim, S. W. Thermochimica Acta 1998, 323, 37.
27. Dutta, A.; Pyan, M. E. J Appl Polym Sci 1979, 24, 635.
28. Peggy, C.; Su-Don, H. Polymer 1986, 27, 1183.